A new macro-imager based on Tpx3Cam optical camera for PLIM applications

Sen, Rajannya, Zhdanov, Alexander, Hirvonen, Liisa, Svihra, Peter, Andersson-Engels, Stefan, et al.

Rajannya Sen, Alexander Zhdanov, Liisa M. Hirvonen, Peter Svihra, Stefan Andersson-Engels, Andrei Nomerotski, Dmitri Papkovsky, "A new macro-imager based on Tpx3Cam optical camera for PLIM applications," Proc. SPIE 11359, Biomedical Spectroscopy, Microscopy, and Imaging, 113591N (1 April 2020); doi: 10.1117/12.2555387

SPIE.

Event: SPIE Photonics Europe, 2020, Online Only, France

A new macro-imager based on Tpx3Cam optical camera for PLIM applications.

Rajannya Sen[1*], Alexander Zhdanov[1], Liisa M. Hirvonen[2], Peter Svihra[3,4], Stefan Andersson-Engels[5], Andrei Nomerotski[6], Dmitri Papkovsky[1,5*]
[1]School of Biochemistry and Cell Biology, University College Cork, Cork, Ireland; [2]Centre for Microscopy, Characterisation and Analysis (CMCA), The University of Western Australia, Crawley WA 6009, Australia; [3]Department of Physics, Faculty of Nuclear Sciences and Physical Engineering, Czech Technical University, Prague 115 19, Czech Republic; [4]Department of Physics and Astronomy, School of Natural Sciences, The University of Manchester, Manchester M139PL, United Kingdom; [5]Irish Photonics Integration Centre, Tyndall National Institute, Cork, Ireland; [6]Physics Department, Brookhaven National Laboratory, Upton, New York, 11973 USA.

ABSTRACT

The recently designed Tpx3Cam camera based PLIM (Phosphorescence Lifetime IMaging) macro-imager was tested using an array of phosphorescent chemical and biological samples. A series of sensor materials prepared by incorporating the phosphorescent O_2-sensitive dye, PtBP, into five polymers with different O_2 permeability were imaged along with several commercial and non-commercial sensors based on PtBP and PtOEPK dyes. The PLIM images showed good lifetime contrast between the different materials, and phosphorescence lifetime values obtained were consistent with those measured by alternative methods. A panel of live tissues samples stained with PtBP based nanoparticle probe were also prepared and imaged under resting conditions and upon inhibition of respiration. The macro-imager showed promising results as a tool for PLIM of O_2 in chemical and biological samples.

Keywords: Oxygen Sensing and Imaging; Fluorescence and Phosphorescence Lifetime Imaging (FLIM and PLIM); Time Correlated Single Photon Counting (TCSPC); Tpx3Cam camera

1. INTRODUCTION

Fluorescence Lifetime IMaging (FLIM) is actively used in biomedicine, material science, chemistry, cell biology and other applications[1–3]. FLIM measures fluorescent decay time of endogenous or exogenous fluors which produce lifetime response to an analyte of interest or microenvironment. The main advantage of FLIM is that it is essentially independent of the fluor concentration and photobleaching, fluctuations in excitation intensity and detector sensitivity, optical properties of the sample and measurement geometry. FLIM also has internal referencing capabilities and therefore, can produce quantitative, accurate and calibration-free measurements of key biochemical and environmental parameters, such as pH, Ca^{2+}, glucose dynamics, etc[4–8]. While FLIM usually measures short-lived fluors with nanosecond lifetimes, Phosphorescent Lifetime IMaging (PLIM)[9] measures lifetimes in the μs-ms range. Therefore, measured parameters and applications for PLIM differ from those of FLIM. PLIM is particularly useful for quenched-phosphorescent sensing and imaging of molecular oxygen (O_2) in various chemical and biological samples.

Interest in PLIM has increased in the last years with the development of new phosphorescence based materials and applications[10–13]. It is largely being used in the field of biology to determine oxygenation and O_2 consumption in living tissue samples[14–17]. The common detection modalities for PLIM and FLIM include Time Correlated Single Photon Counting (TCSPC) which uses the raster scanning technique. Since long (ms range) pixel dwell times are required to record the long-lived phosphorescence, TCSPC leads to longer image acquisition times for PLIM applications[3,18,19]. Fast gated CCD/CMOS cameras can also be used for wide-field FLIM and PLIM, but such systems are not single photon sensitive and limited by the camera frame rate[3,20–25]. Wide-field TCSPC-FLIM with single photon avalanche photodiode (SPAD) arrays allows single photon detection but needs improvements in detection efficiency, array density and dark count rate[26].

*rajannya.sen@ucc.ie; phone +353 (0)831769811

Biomedical Spectroscopy, Microscopy, and Imaging, edited by Jürgen Popp, Csilla Gergely, Proc. of SPIE Vol. 11359, 113591N · © 2020 SPIE
CCC code: 0277-786X/20/$21 · doi: 10.1117/12.2555387

Moreover, while microscopic imaging is used extensively, macroscopic imaging is less common, despite the high need for quantitative imaging of large biological models has increased in recent times. The existing macroscopic imagers are mostly intensity based and lack FLIM/PLIM capabilities[27]. The PLIM/FLIM macro-imager developed by Becker and Hickl (Germany) for large samples[28] still uses confocal scanning and hence requires long image acquisition times for phosphorescent dyes.

Recently, a new imager based on the Tpx3Cam camera (Amsterdam Scientific Instruments (ASI)) has been developed that allows parallel single photon detection and time stamping in each pixel. The Tpx3Cam is based on a novel silicon optical sensor[29–31] and Timepix3 readout chip[32]. It has a high quantum efficiency within 400-1000 nm, with time resolution of 1.6 ns and frame rate greater than 500 MHz. Coupled with an image intensifier, Tpx3cam can record the arrival time and photon flux at each pixel simultaneously. The camera is data driven and is based on the SPIDR (Speedy PIxel Detector Readout) system[33]. Excellent performance of Timepix and Timepix3 chips has already been demonstrated in a variety of applications, both for the direct charge detection and in optical regime[34–39].

Lately, the Tpx3Cam has been configured into a simple PLIM macro-imager setup[41]. To achieve single photon sensitivity the camera was coupled to a Cricket® adapter with inbuilt image intensifier. Emission filter and lens was coupled to the cricket unit. A super-bright red LED was used to provide pulsed excitation to image 18×18 mm sample area. The resulting system has a compact and flexible design, similar to a standard photographic camera. The imager underwent a basic characterization with planar phosphorescent O_2 sensors and a resolution plate mask. The spatial resolution of the system was assessed using several image acquisition and image processing algorithms to optimise the resolution and performance of the system for the wide-field PLIM. The resolving power was found to be 12.7 lp/mm with line width of 39.4 μm[41]. The instrument response function (IRF) was also measured, which gave a temporal resolution of the system of 30.6 ns (FWHM)[41].

In this study we aimed to further investigate the fast macroscopic wide-field PLIM imager and demonstrate its utility in several important applications. Thus, it was used to characterize an array of homemade, commercial and non-commercial phosphorescent solid-state materials designed for the lifetime-based sensing of O_2, and a set of biological samples comprising live tissue stained with a O_2 sensitive phosphorescent probe. The performance and accuracy of the PLIM and lifetime measurements were analysed and compared with alternative O_2 measurement and imaging systems.

2. METHODS

2.1 Materials

Polystyrene (PS), poly(methyl methacrylate) (PMMA), polyvinyl chloride (PVC) and poly(vinylidene chloride) (PVDC) polymers were from Sigma-Aldrich, hydrogel D4 was from Degussa. Pt (II)-benzoporphyrin dye (PtBP) was provided by Luxcel Biosciences. The commercial O_2 sensors were from Mocon (Optech® stickers[42]) and Pyroscience[43]. The LDPE and PLA based PtBP sensors [44] and PtOEPK-PS sensor spotted on microporous membrane and filter paper[45,46] were prepared as described in the corresponding papers.

Antimycin A (Complex III inhibitor), NaN3 (Complex IV inhibitor) and DMEM media were from Sigma-Aldrich, plasticware was from Sarstedt (Ireland). The NanO2-IR probe (10 mg/mL stock in H_2O) was from Luxcel Biosciences (Cork, Ireland), Working solution of NanO2-IR (1 mg/mL) was prepared by diluting the stock with DMEM media supplemented with 10 mM glucose, 2 mM L-glutamine and 10 mM HEPES (pH=7.2), immediately prior to use.

2.2 PLIM macro-imager setup

The design of the Tpx3Cam PLIM macro-imager is described elsewhere[41]. Briefly, the Cricket® adapter with inbuilt image intensifier, power supply and back-end relay optics (Photonis, Merignac, France), and a 760 nm bandpass emission filter (25 mm, Edmund Optics, York, UK) provided a compact and flexible design to the imager. The Tpx3Cam was coupled to one end of the Cricket® and a 50 mm Navitar NMV-50M11" lens to the other. The imager was placed in an upright position, such that it can image the samples placed at a distance of ~80 mm from the lens. The block-diagram of the setup is shown in Figure 1. A 5 mm super-bright red LED with central wavelength at 627 nm (Parts Express, Springboro, OH) was used to excite the samples. The LED was operated in a pulsed mode which was synchronized with the camera by two pulse generators. To control the temperature of the samples, a dry bath/block heater (Thermo Fisher Scientific, Carlsbad,

CA) was used, which was normally set up at 37ºC. The system was enclosed in a black box to protect it from the ambient light.

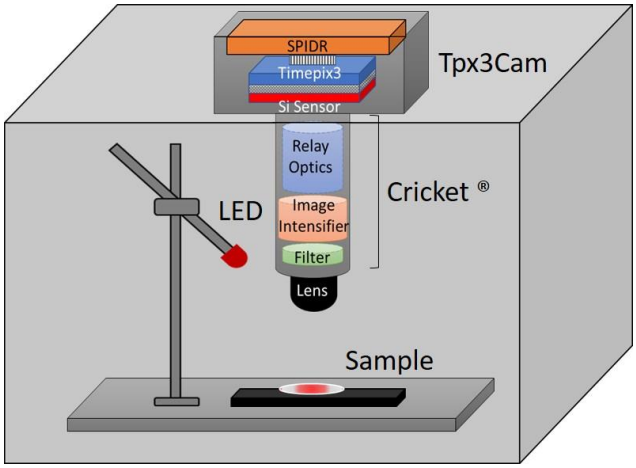

Figure 1. Experimental setup of the Tpx3Cam imager showing its upright orientation.

2.3 Data processing

The operational parameters, alignment and focus of the system was tuned by the Sophy™ software provided by ASI. A custom-designed software was used to acquire the raw data from the Tpx3Cam imager in a binary format. The data was processed by a C-language program with sub-pixel centroiding[41,47]. TRI2 software was used to fit the resulting data matrix for each camera pixel with two-exponential function to determine lifetime values.

2.4 Sample preparation

An array of phosphorescent coatings based on Polystyrene (PS), poly(methyl methacrylate) (PMMA), polyvinyl chloride (PVC) and poly(vinylidene chloride) (PVDC) were prepared from the corresponding cocktails. Each cocktail, which contained 0.25 mg/ml of Pt (II)-benzoporphyrin (PtBP), 5% w/w of the polymer in tetrahydrofuran (THF), was spotted on 2x2 cm pieces of polyester film, 70 µm thick (Mylar®, Du Pont). Seven serial 1:3 dilutions of each dye were prepared and spotted in a similar manner. Other forms of PtBP sensors spotted on microporous PVDF membrane (Millipore) and absorbed in silicon glass beads were also produced.

For the preparation of the biological samples, protocols involving animals were approved by the University College Cork Animal Experimentation Ethics Committee, and all the experiments were conducted under the license from the Irish Government in accordance with national and EU legislation (European Directive 2010/63/EU). On the day of the experiment, 4-week-old AE19130/1276 female mice (Envigo, UK) were sacrificed, fresh tissue samples of large and small intestine were quickly dissected, washed with PBS and placed in DMEM media equilibrated at 37ºC. One set of the extracted tissues was then transferred into mini-dishes and submerged into 2 ml of DMEM containing NanO2-IR (1 mg/ml) for 30 min for surface staining. The other set of tissues submerged in dye in a similar manner was treated with AntA/NaN3 inhibitors of respiration for 30 min before imaging. The experiments with the treated and untreated samples were repeated three times with identical tissue samples to confirm the consistency of the data.

3. RESULT AND DISCUSSION

3.1 Imaging of the different senor materials

The series of homemade polymeric phosphorescent coatings spotted on the polyester films were first imaged with the Tpx3Cam imager. Each spot contained ~83 ng of PtBP dye. The image was acquired under normal air conditions (22ºC, 20.86% O_2) with LED at 4V and 50 ns pulse width and 20 s integration time. The intensity and the PLIM images of the sensor film are shown in Figure 2a and 2b respectively. The intensity images (Figure 2a) showed the significant fluctuations

in the optical signal across each spot, so they did not show the clear differences in their luminescence quenching. Conversely, the PLIM images (Figure 2b) showed much better stability of the lifetime signals and excellent contrast between the different polymers.

To deoxygenate the coatings, the same film with spotted sensors was soaked in a phosphate-sulfite buffer. The intensity and PLIM images acquired are shown in Figure 2c, d. As expected, the difference in lifetime values and contrast between the different sensor coatings was largely reduced, and the lifetime signals for all the sensors approached ~50 µs, which corresponds to the unquenched lifetime of PtBP. It should be noted that during the preparation of the sensor samples, one coating (PS based) detached from the film support as a result of the rough handling, so it could not be imaged and seen on Fig. 2c,d.

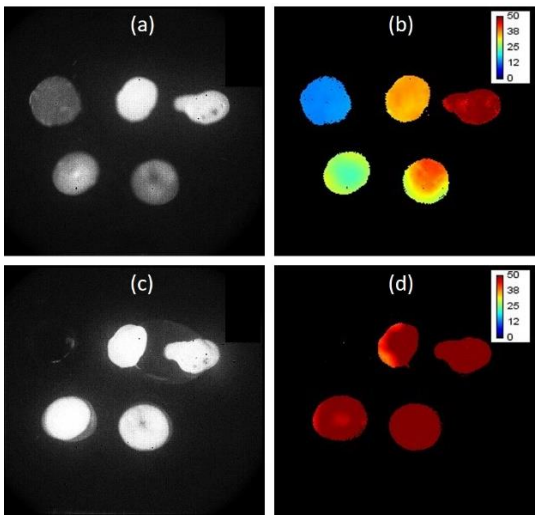

Figure 2. Images of the polymer based phosphorescent coating spotted on polyester film (spot size~ 2-3 mm): in the oxygenated state in (a) intensity and (b) lifetime(µs) scale; in the de-oxygenated state in (c) intensity and (d) PLIM (µs) mode, 22ºC.

To determine the sensitivity of the imager, the phosphorescent coatings containing different dilutions of PtBP dye (1:3 serial dilutions) in PS spotted on the polyester film were imaged under the ambient temperature and oxygenation conditions (22ºC, 20.86% O_2). The amount of the dye per spot ranged from 250-0.34 ng (serial 3-fold dilutions). The Tpx3Cam imager was sensitive to the first 5 dilutions and Figure 3 represents the variation in the intensity and lifetime recorded for these spots. While there was a variation in the intensity, the lifetime remained stable at decreasing concentrations.

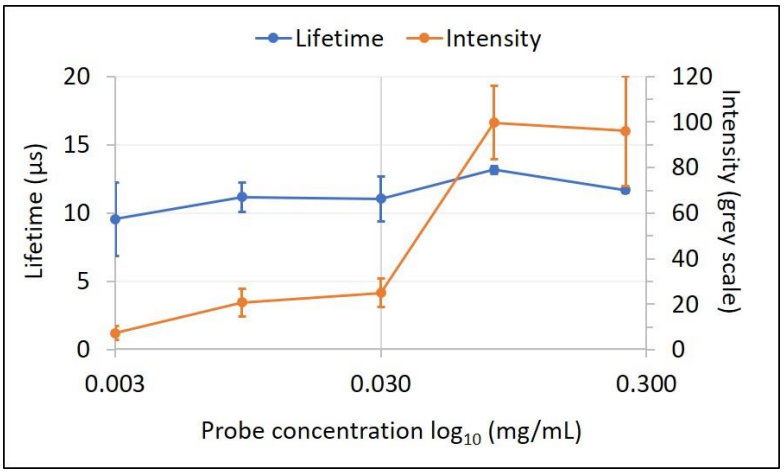

Figure 3. Variation of the intensity and lifetime for Polystyrene based PtBP dye with increasing dilutions.

Several other commercial and non-commercial sensors based on PtBP dye were also imaged under normal conditions, using the LED power 4V, pulse width 50 nm and integration time 20 s. Figure 4a shows photographic images of the different sensors, while Figure 4b shows their PLIM images. The PVDF membrane (12.9±0.9 µs), bead sensor (13.3±0.4 µs) and the sensor from Pyroscience (13.5±0.6 µs) all showed similar lifetime values and variability (S.D.), whereas higher lifetime values were noted for the Optech® sensor (15.4±0.4 µs) and for the membrane sheet (19.9±0.07 µs).

The extruded LDPE and PLA sensor pellets and films based on the PtBP phosphor (Figure 4c) were also analysed, under the same optical settings. The PLIM images of the sensors are shown in Figure 4d. The PLA pellet and film in Figure 4d cannot be differentiated due to thresholding limits. The lifetime values for the PLA sensors (36.5±0.4 µs) was significantly higher than for the LDPE sensors (13.7±0.1 µs), in agreement with the reported data[44].

The PtOEPK-PS based O_2 sensors[48], which are spectrally compatible with the Tpx3Cam set-up, were also imaged. Their photographic and PLIM images are shown in Figure 4e,f, respectively. The two different sensor types (spots on filter paper and PVDF membrane support) produced similar mean lifetimes and standard deviation of 15.8±0.2 µs and 15.4±0.15 µs respectively. These results are also consistent with other reported data[45,46].

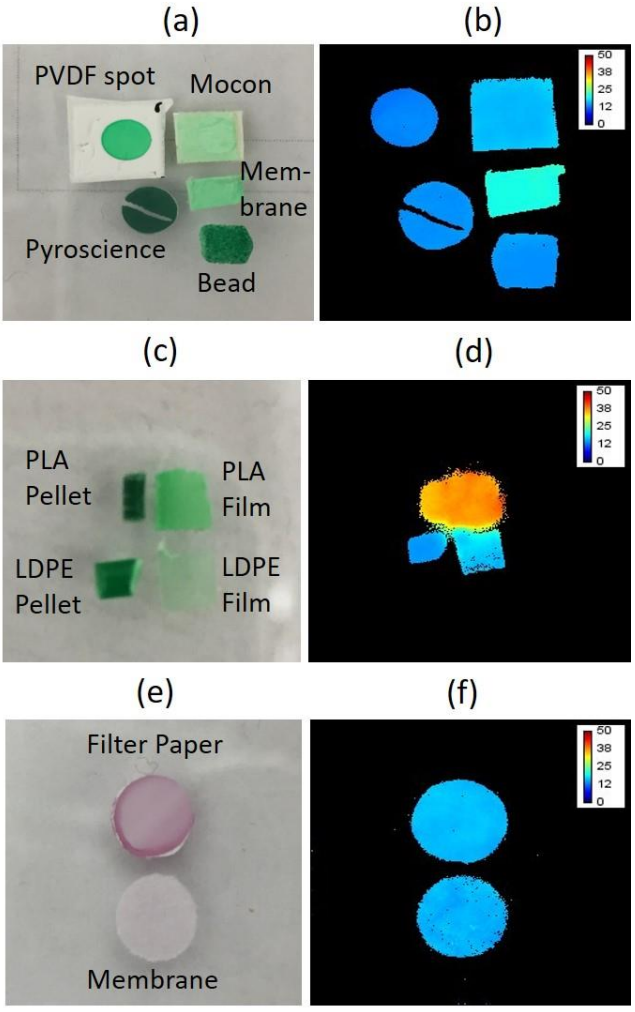

Figure 4. Sets of commercial and custom-made O_2 sensors imaged with the Tpx3Cam imager. (a) Photograph and (b) PLIM image of the PtBP based sensors in various forms; (c) Photograph and (d) PLIM image of LDPE-PLA based PtBP sensors and (e) Photograph and (f) PLIM image of the two PtOPEK based sensors.

3.2 Biological samples

Several live tissue samples isolated from mice (post-mortem) were stained with the soluble phosphorescent probe, NanO2-IR, and then imaged. For these physiological measurements the temperature-controlled stage was set at 37ºC. The photograph of the specimen of a large intestine is shown in Figure 5a and the corresponding intensity images in Figure 5b. The respective PLIM images of the untreated (respiring) and treated (with blocked mitochondrial respiration) large intestine are shown in Figure 5c,d. Although there is no drastic change in the color of the two PLIM images, the small shift in lifetime values clearly reflects the difference in respiration for the two tissue samples. The regions of higher lifetimes in Figure 5c inform on the level of depletion of local O_2 due to cell respiration. The boxplot in Figure 5e shows that the inhibitors had a lower effect on this tissue sample but still there is a prominent shift in the median lifetime value (24.41 µs and 20.55 µs for the treated and untreated samples, respectively).

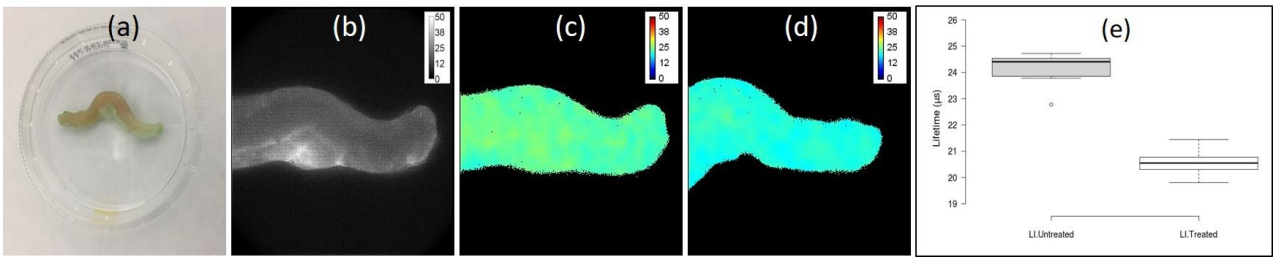

Figure 5. Images of the samples of a large intestine stained with NanO2-IR probe by the topical application: (a) Photograph, (b) intensity images and PLIM images of the (c) respiring and (d) non-respiring tissue samples. (e) Boxplots representing the comparison between the median lifetimes of the treated and untreated large intestine (LI) samples from mice (10 values each).

Thus, we can conclude that the imager recognizes small physiologically relevant shifts in the lifetime values of O_2 sensitive probes; a longer staining period for the biological samples is expected to produce better lifetime contrast between samples. Upon proper calibration of the probe, the map of O_2 distribution within this biological sample can be obtained by converting the lifetime values into O_2 concentrations.

4. CONCLUSION

A series of homemade solid-state phosphorescent O_2 sensors based on PtBP and PtOEPK phosphorescent dyes embedded in the different polymers were imaged on the new PLIM macro-imager, along with the other commercial and non-commercial sensors, using image acquisition time of 20 seconds. The different sensor materials showed high brightness and good lifetime contrast due to the different selection of polymers. The lifetime values obtained for the other sensors were in agreement with their previous studies. PLIM of the sensors with progressively increasing dilutions of the phosphorescent dye and decreasing optical signals from the coating demonstrated their high sensitivity and stability. The initial PLIM applications with ex-vivo samples of live animal tissue also showed promising results, despite of the much weaker phosphorescence intensity signals. Tissue treatment with model inhibitors of respiration produced the anticipated changes in lifetime values: shorter lifetimes for non-respiring samples.

Overall, the new macro-imager based on Tpx3Cam demonstrated good functionality and operational performance, and it looks promising for PLIM applications including in vivo imaging of tissue oxygenation. The Cricket® adapter couples the camera with the image intensifier and optical lens. This provides proper rigid alignment of the key optoelectronic components and produces a compact and flexible measurement unit for PLIM. The imager has fast data acquisition time (~a few seconds), can image objects up to several centimeters in size with high spatial resolution and flexible geometry (vertical, horizontal and tilted configurations are possible). The system is well-suited for various biomedical applications compatible with wide-field PLIM. Its initial characterization with ex-vivo tissue samples provide evidence that it can be applied to biological samples in vivo and can be used in physiological studies with various tissue and disease models.

Acknowledgement: *Financial support of this work by the Science Foundation Ireland, grants SFI/12/RC/2276_P2 and SFI/17/RC-PhD/3484, is gratefully acknowledged. Authors are grateful to Dr. Patrick Fitzgerald for supplying the biological samples.*

REFERENCES

[1] Korczyński, J. and Włodarczyk, J., "Fluorescence lifetime imaging microscopy (FLIM) in biological and medical research," Postepy Biochem. **55**(4), 434–440 (2009).

[2] Marcu, L., "Fluorescence lifetime techniques in medical applications," Ann. Biomed. Eng. **40**(2), 304–331 (2012).

[3] Becker, W., "Fluorescence lifetime imaging - techniques and applications," J. Microsc. **247**(2), 119–136 (2012).

[4] Orte, A., Alvarez-Pez, J. M. and Ruedas-Rama, M. J., "Fluorescence lifetime imaging microscopy for the detection of intracellular pH with quantum dot nanosensors," ACS Nano **7**(7), 6387–6395 (2013).

[5] Zheng, K., Jensen, T. P. and Rusakov, D. A., "Monitoring intracellular nanomolar calcium using fluorescence lifetime imaging," Nat. Protoc. **13**(3), 581–597 (2018).

[6] Veetil, J. V, Jin, S. and Ye, K., "Fluorescence lifetime imaging microscopy of intracellular glucose dynamics" (2012).

[7] Agronskaia, A. V., Tertoolen, L. and Gerritsen, H. C., "Fast fluorescence lifetime imaging of calcium in living cells," J. Biomed. Opt. **9**(6), 1230 (2004).

[8] Lakowicz, J. R., Szmacinski, H., Nowaczyk, K. and Johnson, M. L., "Fluorescence lifetime imaging of calcium using Quin-2," Cell Calcium **13**(3), 131–147 (1992).

[9] Chelushkin, P. S. and Tunik, S. P., "Phosphorescence Lifetime Imaging (PLIM): State of the Art and Perspectives," [Progress in Photon Science], Springer, 109–128 (2019).

[10] Papkovsky, D. B., "Methods in optical oxygen sensing: protocols and critical analyses," [Methods in enzymology], Elsevier, 715–735 (2004).

[11] Tsytsarev, V., Akkenti, F., Pumbo, E., Tang, Q., Chen, Y., Erzurumlu, R. S. and Papkovsky, D. B., "Planar implantable sensor for in vivo measurement of cellular oxygen metabolism in brain tissue," J. Neurosci. Methods **281**, 1–6 (2017).

[12] Banerjee, S., Kuznetsova, R. T. and Papkovsky, D. B., "Solid-state oxygen sensors based on phosphorescent diiodo-borondipyrromethene dye," Sensors Actuators, B Chem. **212**, 229–234 (2015).

[13] Banerjee, S., Arzhakova, O. V., Dolgova, A. A. and Papkovsky, D. B., "Phosphorescent oxygen sensors produced from polyolefin fibres by solvent-crazing method," Sensors Actuators, B Chem. **230**(March), 434–441 (2016).

[14] Fercher, A., Borisov, S. M., Zhdanov, A. V., Klimant, I. and Papkovsky, D. B., "Intracellular O2 sensing probe based on cell-penetrating phosphorescent nanoparticles," ACS Nano **5**(7), 5499–5508 (2011).

[15] Jenkins, J., Dmitriev, R. I. and Papkovsky, D. B., "Imaging cell and tissue O 2 by TCSPC-PLIM," [Advanced Time-Correlated Single Photon Counting Applications], Springer, 225–247 (2015).

[16] Dmitriev, R. I. and Papkovsky, D. B., "Optical probes and techniques for O 2 measurement in live cells and tissue," Cell. Mol. life Sci. **69**(12), 2025–2039 (2012).

[17] Zhdanov, A. V., Okkelman, I. A., Golubeva, A. V., Doerr, B., Hyland, N. P., Melgar, S., Shanahan, F., Cryan, J. F. and Papkovsky, D. B., "Quantitative analysis of mucosal oxygenation using ex vivo imaging of healthy and inflamed mammalian colon tissue," Cell. Mol. Life Sci. **74**(1), 141–151 (2017).

[18] Phillips, D. and Christensen, R. L., "Time Correlated Single-Photon Counting (Tcspc) Using Laser Excitation," Instrum. Sci. Technol. **14**(3–4), 267–292 (1985).

[19] Becker, W., "3 Advanced TCSPC-FLIM techniques" (2018).

[20] Hirvonen, L. M. and Suhling, K., "Wide-field TCSPC: Methods and applications," Meas. Sci. Technol. **28**(1) (2017).

[21] Hirvonen, L. M., Petrášek, Z., Beeby, A. and Suhling, K., "Sub-μs time resolution in wide-field time-correlated single photon counting microscopy obtained from the photon event phosphor decay," New J. Phys. **17** (2015).

[22] Hirvonen, L. M., Festy, F. and Suhling, K., "Wide-field time-correlated single-photon counting (TCSPC) lifetime microscopy with microsecond time resolution," Opt. Lett. **39**(19), 5602 (2014).

[23] Wei, L., Yan, W. and Ho, D., "Recent advances in fluorescence lifetime analytical microsystems: Contact optics and CMOS time-resolved electronics," Sensors (Switzerland) **17**(12) (2017).

[24] Sparks, H., Görlitz, F., Kelly, D. J., Warren, S. C., Kellett, P. A., Garcia, E., Dymoke-Bradshaw, A. K. L., Hares, J. D., Neil, M. A. A., Dunsby, C. and French, P. M. W., "Characterisation of new gated optical image intensifiers for fluorescence lifetime imaging," Rev. Sci. Instrum. **88**(1) (2017).

[25] Petrášek, Z. and Suhling, K., "Photon arrival timing with sub-camera exposure time resolution in wide-field time-resolved photon counting imaging," Opt. Express **18**(24), 24888 (2010).

[26] Gersbach, M., Trimananda, R., Maruyama, Y., Fishburn, M., Stoppa, D., Richardson, J., Walker, R., Henderson, R. K. and Charbon, E., "High frame-rate TCSPC-FLIM using a novel SPAD-based image sensor," Detect. Imaging Devices Infrared, Focal Plane, Single Phot. **7780**(May 2014), 77801H (2010).
[27] Zarychta-Wiśniewska, W., Burdzinska, A., Zagozdzon, R., Dybowski, B., Butrym, M., Gajewski, Z. and Paczek, L., "In vivo imaging system for explants analysis—A new approach for assessment of cell transplantation effects in large animal models," PLoS One **12**(9), 1–21 (2017).
[28] Chelushkin, P. S. and Tunik, S. P., [Progress in Photon Science], Springer International Publishing (2017).
[29] Fisher-Levine, M. and Nomerotski, A., "TimepixCam: A fast optical imager with time-stamping," J. Instrum. **11**(3) (2016).
[30] Nomerotski, A., Chakaberia, I., Fisher-Levine, M., Janoska, Z., Takacs, P. and Tsang, T., "Characterization of TimepixCam, a fast imager for the time-stamping of optical photons," J. Instrum. **12**(1) (2017).
[31] Nomerotski, A., "Imaging and time stamping of photons with nanosecond resolution in Timepix based optical cameras," Nucl. Instruments Methods Phys. Res. Sect. A Accel. Spectrometers, Detect. Assoc. Equip. **937**(May), 26–30 (2019).
[32] Poikela, T., Plosila, J., Westerlund, T., Campbell, M., Gaspari, M. De, Llopart, X., Gromov, V., Kluit, R., Beuzekom, M. Van, Zappon, F., Zivkovic, V., Brezina, C., Desch, K., Fu, Y. and Kruth, A., "Timepix3: A 65K channel hybrid pixel readout chip with simultaneous ToA/ToT and sparse readout," J. Instrum. **9**(5) (2014).
[33] Visser, J., Beuzekom, M. Van, Boterenbrood, H., Heijden, B. Van Der, Muñoz, J. I., Kulis, S., Munneke, B. and Schreuder, F., "SPIDR: A read-out system for Medipix3 & Timepix3," J. Instrum. **10**(12) (2015).
[34] Zhao, A., Van Beuzekom, M., Bouwens, B., Byelov, D., Chakaberia, I., Cheng, C., Maddox, E., Nomerotski, A., Svihra, P., Visser, J., Vrba, V. and Weinacht, T., "Coincidence velocity map imaging using Tpx3Cam, a time stamping optical camera with 1.5 ns timing resolution," Rev. Sci. Instrum. **88**(11) (2017).
[35] Ianzano, C., Svihra, P., Flament, M., Hardy, A., Cui, G., Nomerotski, A. and Figueroa, E., "Spatial characterization of photonic polarization entanglement using a Tpx3Cam intensified fast-camera," 1–22 (2018).
[36] Debrah, D. A., Stewart, G. A., Basnayake, G., Nomerotski, A., Svihra, P., Lee, S. K. and Li, W., "Developing a camera-based 3D momentum imaging system capable of 1 Mhits/s," Rev. Sci. Instrum. **91**(2) (2020).
[37] Roberts, A., Svihra, P., Al-Refaie, A., Graafsma, H., Küpper, J., Majumdar, K., Mavrokoridis, K., Nomerotski, A., Pennicard, D., Philippou, B., Trippel, S., Touramanis, C. and Vann, J., "First demonstration of 3D optical readout of a TPC using a single photon sensitive Timepix3 based camera," J. Instrum. **14**(6) (2019).
[38] Zhang, Y., England, D., Nomerotski, A., Svihra, P., Ferrante, S., Hockett, P. and Sussman, B., "Multidimensional quantum illumination via direct measurement of spectro-temporal correlations," 1–9 (2019).
[39] Vallerga, J., Tremsin, A., Defazio, J., Michel, T., Alozy, J., Tick, T. and Campbell, M., "Optical MCP image tube with a quad Timepix readout: Initial performance characterization," J. Instrum. **9**(5) (2014).
[40] Roberts, A., Svihra, P., Al-Refaie, A., Graafsma, H., Küpper, J., Majumdar, K., Mavrokoridis, K., Nomerotski, A., Pennicard, D., Philippou, B., Trippel, S. and Vann, J., "First demonstration of 3D optical readout of a TPC using a single photon sensitive Timepix3 based camera" (2018).
[41] Sen, R., Hirvonen, L. M., Zhdanov, A., Svihra, P., Andersson-Engels, S., Nomerotski, A. and Papkovsky, D., "New luminescence lifetime macro-imager based on a Tpx3Cam optical camera," Biomed. Opt. Express **11**(1), 77 (2020).
[42] "MOCON.", Available online, <https://www.mocon.com/instruments/optech-o2-model-p.html>.
[43] "Pyroscience.", <https://www.pyroscience.com/contactless-fiber-optic-oxygen-sensor-spots.html>.
[44] Kelly, C., Yusufu, D., Okkelman, I., Banerjee, S., Kerry, J. P., Mills, A. and Papkovsky, D. B., "Extruded phosphorescence based oxygen sensors for large-scale packaging applications," Sensors Actuators B Chem., 127357 (2019).
[45] Smiddy, M., Fitzgerald, M., Kerry, J. P., Papkovsky, D. B., O' Sullivan, C. K. and Guilbault, G. G., "Use of oxygen sensors to non-destructively measure the oxygen content in modified atmosphere and vacuum packed beef: Impact of oxygen content on lipid oxidation," Meat Sci. **61**(3), 285–290 (2002).
[46] Papkovsky, D. B., Smiddy, M. A., Papkovskaia, N. Y. and Kerry, J. P., "Nondestructive measurement of oxygen in modified atmosphere packaged hams using a phase-fluorimetric sensor system," J. Food Sci. **67**(8), 3164–3169 (2002).
[47] Hirvonen, L. M., Fisher-Levine, M., Suhling, K. and Nomerotski, A., "Photon counting phosphorescence lifetime imaging with TimepixCam," Rev. Sci. Instrum. **88**(1) (2017).
[48] Papkovsky, D. B., Ponomarev, G. V., Trettnak, W. and O'Leary, P., "Phosphorescent Complexes of Porphyrin Ketones: Optical Properties and Application to Oxygen Sensing," Anal. Chem. **67**(22), 4112–4117 (1995).